Moritoring Wingter Wheat Growth With Grand Based Microwave Radiometers (GBMR)

Hui LU, Toshio KOIKE, Hiroyuki TSUTSUI, Tobias GRAF and David Ndegwa KURIA
Department of Civil Engineering,
The University of Tokyo
7-3-1 Hongo, Bunkyo-ku, Tokyo, 113-8656, Japan
lu@hydra.t.u-tokyo.ac.jp

Abstract— **From November 2006 to June 2007 a field experiment 'Tanashi Experiment' was conducted in a farm of the University of Tokyo, Japan. Continuous ground measurements of meteorological variables, soil moisture and temperature profiles and vegetation status have been taken. At the same time, the ground based microwave radiometers (GBMR) are employed to provide accurate field measurements of brightness temperature up-welling from the plot, at the frequencies of 6.925, 10.65, 18.7, 23.8, 36.5 and 89 GHz. The scientific objectives are presented in this paper and the corresponding experiment set-up is described. The influences of vegetation layer on the brightness of various frequencies are analyzed. The TB of all frequencies and polarization is found to be saturated and reach same values when vegetation water content larger than 4 kg/m^2. Based on the analysis of winter wheat experiment results, the Polarization Index (PI) of 6.9GHz and the Index of Soil Wetness (ISW) calculated from 18GHz and 6.9GHz horizontal polarization were recommended to compose the look up table. Potential applications of this winter wheat microwave radiometer observation are the development and validation of land surface variables retrieval algorithm and the study of land surface process and the land atmosphere interaction, and.**

***Keywords-** passive microwave remote sensing; vegetation water content ; brightness temperature; field experiment; ground based microwave radiometer*

I. INTRODUCTION

Researches related to earth system modeling, global scale environmental processes monitoring and climate changing studying are conducted using globally measured parameters, such as the soil moisture, soil temperature and vegetation water content. Among them, the primary one is the soil moisture, which links the land surface and atmosphere by influencing the exchange of energy and material between these two parts. However, due to its large variability, it is very difficult to observe the spatial and temporal distribution of soil moisture in a large scale by in situ measurements, which are both time consuming and expensive. As a result, in recent 30 years, much effort has been directed towards observing soil moisture by satellite remote sensing approaches. Fortunately, satellite passive microwave remote sensing offers a possibility to measure such an important variable at the global scale, by directly measuring the dielectric properties which are strongly related to the liquid moisture content. Moreover, extra advantages of passive microwave remote sensing include long wavelength in microwave region and independent of illumination source. These characteristics have been recognized by many scientists and large research activities have been carried out in the past 30 years.

Currently, globally soil moisture products are mainly retrieved from C band and X band observation [1]. And in order to get time continuous information about soil moisture and land surface energy budget, land surface data assimilation systems are developed. But there are still some problems left to be solved, such as retrieval soil moisture from higher frequency bands (19GHz and 37GHz) observation, counting the vegetation effects on different frequencies, and the parameterization problems inside the land data assimilation systems.

In order to improve our understanding of the radiative transfer process taken place on the land surface and to improve our capability to model land surface processes, a long term field experiment was designed to monitor the growth cycle of winter wheat, and have been carried out from November 2006 to June 2007 in the Field Production Science Center in Graduate School of Agricultural and Life Sciences in the University of Tokyo (UTFPSC), Tokyo, Japan.

In this paper, we present the objectives and the overall set-up of the 'Tanashi experiment' at the second section. In section 3, some radiometric characteristics of winter wheat were explored through microwave observations at the frequencies operating by the Advanced Microwave Scanning Radiometers for EOS (AMSR-E) (6.925GHz, 10.65GHz, 18.7GHz, 23.8GHz, 36.5GHz and 89GHz). Finally, we end this paper with some collusion and remark.

II. EXPERIMENT DISCRIPTION

The 'Tanashi Experiment' was designed with the following objective in mind: Improving the understanding of the influences of soil and vegetation on the remote sensing signals at different frequencies and polarizations;

A. *Site Overview*

Figure 1 provides an overview of the instrument set-up. Two Ground Based Microwave Radiometer (GBMR) systems, GBMR-6ch and GBMR-7ch, have been installed at the edge of experiment field. In front of those two radiometers, there are 5 footprints which are the main targets of this field experiment.

Authorized licensed use limited to: Dedan Kimathi University of Technology. Downloaded on November 14,2022 at 07:26:19 UTC from IEEE Xplore. Restrictions apply.

The footprint A and B are the reference bare soil footprint and reference vegetation footprint of GBMR-6ch, respectively. Analogously, footprint E and D are the reference footprints for the another radiometer, i.e. GBMR-7ch. The footprint C, the one in the central location which can be observed by GBMR-6ch and GBMR-7ch simultaneously, is the common footprint.

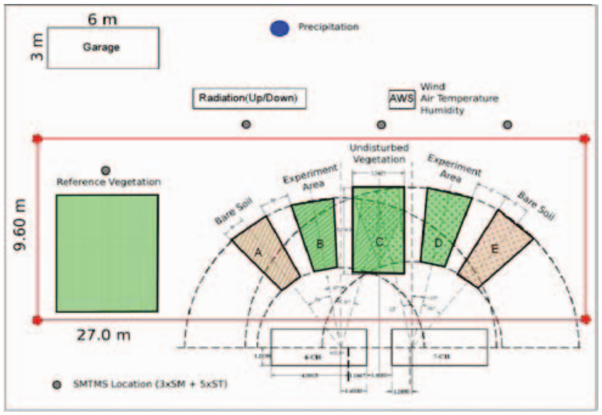

Fig. 1 Overview of Instrument Set-Up

Two different scan areas have been selected to observe the brightness temperature of field in different situations:

Footprint B,C and D – Undisturbed footprint: The plots in this area were undisturbed during whole observation period and therefore it represented the natural status of the field.

Footprint A and E – Reference bare soil footprint: In this area the vegetation was removed regularly to keep the bare soil exposed to radiometers.

Beside those 5 footprints, there is a plot used as vegetation reference site. All of the vegetation sampling procedures were taken here to avoid disturb the natural situation of footprint B, C and D.

The location for soil moisture and temperature measurement system (SMTMS) and the automatic weather station (AWS) have been selected, so that they are close to the radiometer footprints. The radiation station and rainfall gauge are also located close to the footprint to ensure the representativity of meteorological data measurement.

B. *Brightness Temperature Measurment*

The ground based brightness temperature observations have been implemented by means of the 6 channel Ground Based Microwave Radiometer (GBMR-6ch) and 7 channel Ground Based Microwave Radiometer (GBMR-7ch). The GBMR-6ch is a dual polarization, multi-frequency passive microwave radiometer, which observes the brightness temperature at 6.925, 10.65 and 18.7 GHz, while the GBMR-7ch operating at frequencies of 18.7, 23.8, 36.5 and 89GHz with both horizontal and vertical polarizations, with the exception of 23.8GHz which is vertical polarization only. The set of those two radiometers was developed to provide frequencies similar to those of the Advanced Microwave Scanning Radiometers for EOS (AMSR-E) on Aqua and AMSR on ADEOS-II. Details of GBMR-6ch and GBMR-7ch can be found from a former paper of authors [2] and from manuals provided by the manufacturer, RPG [3].

Figure 2 shows a comparison between the brightness temperatures observed at 18.7 GHz by GBMR-6ch and that by GBMR-7ch. The line with triangle represents the results measured by GBMR-6ch, and the line with cycle is those measured by GBMR-7ch. The root mean square error between the GBMR-7ch and GBMR-6ch is 1.74K for vertical polarization (not shown here), and 4.03K for horizontal polarization, respectively. Considering the fact that the calibration scheme is different for GBMR-6ch and GBMR-7ch, and the fact that the observed target is around 300K, the error is negligible. And then, we are sure that both systems were observing same target with same accuracy at same time. Finally, a brightness temperature data set from 6.9GHz up to 89GHz is then created.

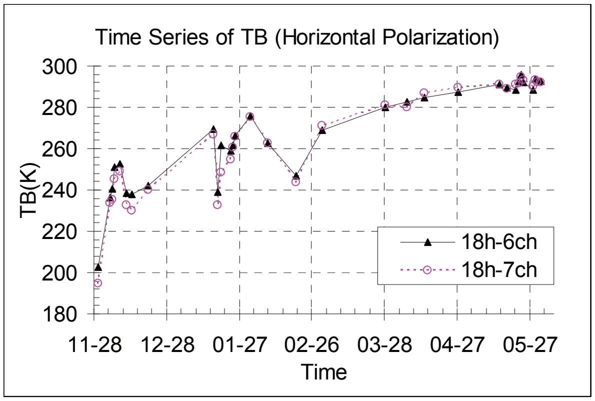

Fig. 2 Comparison of TB observed at 18GHz by GBMR-6ch and GBMR-7ch

C. *Vegetation Measurements Instruments*

Vegetation development was monitoring through measuring the height, biomass, dry matter, water content and LAI. Sampling area of 1*1 m^2 area was selected in the vegetation reference field. Wet biomass was measured just after cutting, and then the wheat was separated into three parts: heads, leaves and stems. Weight and area of each part were measured separately. By summing the area of those three parts, the Leaf Area Index (LAI) was calculated.

A spectroradiometer, ASD FieldSpec Pro, was also used to measure the reflectance at a spectral range of 350nm – 2500nm. The normalized difference vegetation index (NDVI) was calculated by using reflectance values of red bands (620 - 670nm) and Near-Infrared (NIR) bands (841 - 876 nm), the same bands as MODIS products using.

III. OBSEVATION RESULTS AND DISCUSSION

Figure 3 shows the time series of observed vegetation water content (VWC). From this figure, it is clear that the vegetation water content increased slowly during the period from November, 2006 to March, 2007. And after March, the vegetation developed rapidly. The vegetation water content reached the maximum, 4.109kg/m^2, at May 17, 2007. And after maturation, the vegetation water content decreased as winter wheat got drying. The whole experiment therefore can be

Authorized licensed use limited to: Dedan Kimathi University of Technology. Downloaded on November 14,2022 at 07:26:19 UTC from IEEE Xplore. Restrictions apply.

divided into two periods: no vegetation effects period (before March) and vegetated period (after March 28).

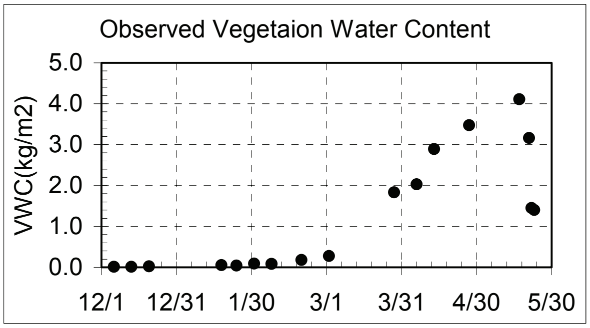

Fig. 3 Time Series of Observed Vegetation Water Content.

A. Vegetation effects on land surface emssion

Figure 4 shows the observed apparent emissivity (equals to the observed brightness temperature divided by the surface temperature) changing as the vegetation water content increasing. Triangles represent the apparent emissivity of vertical polarization, cycles represent horizontal polarization. From figure 4, it is clear that the apparent emissivity increases as vegetation water content increasing, for all frequencies and polarizations. Generally, at same frequency, the emissivity at vertical polarization is larger than that at horizontal polarization, except for 89GHz, at which the emissivity of horizontal polarization is larger than vertical polarization. Moreover, for the frequencies of 6.9GHz, 10GHz, 18GHz and 36GHz, the emissivity of horizontal polarization increases faster than the emissivity of vertical polarization of same frequency. And finally, the emissivity of both polarizations tends to reach the same values.

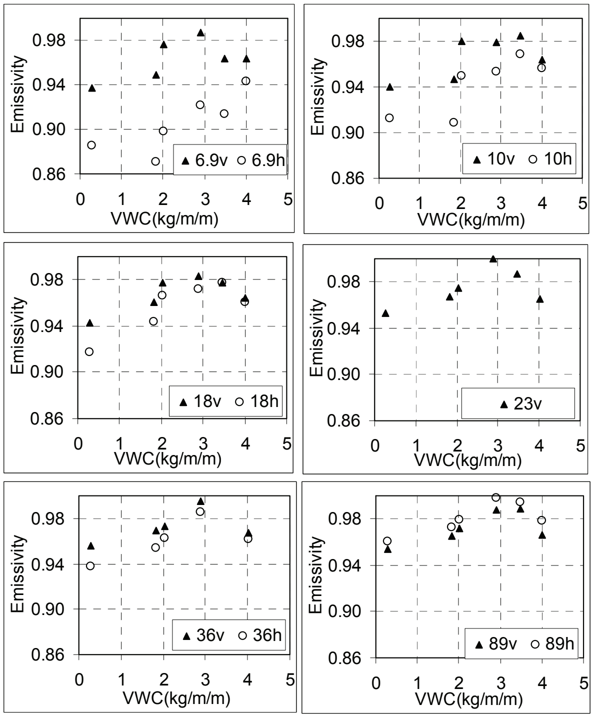

Fig. 4 Variation of observed apparent emissivity due to VWC increase

B. Indentifying the heavy vegetation criterion

By using Jackson's model [4], we can calculate the optical thickness (τ) and transmittivity (L) of vegetation layer as following equations:

$$\tau = b' \times \lambda^{\chi} \times VWC \tag{1}$$

$$L = \exp(-\tau / \cos\theta) \tag{2}$$

where λ is wavelength in cm, VWC is vegetation water content in kg/m^2, θ is incident angle. b' and χ are parameters dependent on the vegetation type. In the case of winter wheat, they are equal to 1.15 and -1.08, respectively.

Table. 1 Transmittivity of vegetation layer

Date	Feb-07	Mar-28	Apr-13	May-17
VWC (kg/m^2) F(GHz)	0.084	1.834	2.894	4.109
6.925	0.97	0.47	0.30	0.18
10.65	0.95	0.30	0.15	0.07
18.7	0.90	0.11	0.03	0.01
23.8	0.88	0.06	0.01	0.00
36.5	0.81	0.01	0.00	0.00
89	0.58	0.00	0.00	0.00

Table 1 shows the calculation results of the transmittivity of vegetation layer at the date of February 7, March 28, April 13 and May 17. From **Table 1**, it is clear that the vegetation effect is small at February 7, giving the facts that the transmittivity is larger than 0.9 for lower frequencies. And after March 28, transmittivity is less than 0.5 for all frequencies. By summarizing results shown in Fig. 5 and table 2, the heavy vegetation criterion, over which the emission from vegetation layer is uniform for all microwave frequencies and polarization, is 2 kg/m^2 for frequencies higher than 18.7GHz. For all frequencies equipped on AMSR-E (including 6.925 and 10.65GHz), this criterion should move to 4.0kg/m^2.

C. Vegetation Effects on Soil Moisture Algorithm

Currently, the RTM proposed by Jackson and Schmugge [4] is used to simulate the vegetation effects in our algorithm. By using the data observed in winter wheat experiment, we can analyze the vegetation effects on our ISW-PI algorithm.

Figure 5 shows a comparison of ISW calculated from various combinations of frequencies. Upper plot shows combinations of vertical polarization, lower plot show combinations of horizontal polarization. Blue diamonds represent the combination between 10GHz and 6GHz; pink rectangles for the combination of 18GHz and 10GHz; and dark red triangles for the combination of 18GHz and 6GHz. From figure 5, it is obvious that the ISW calculated from 18GHz and 6GHz horizontal polarization has the largest variation range as vegetation water content increases from 0.182 to 4.109 kg/m^2.

Authorized licensed use limited to: Dedan Kimathi University of Technology. Downloaded on November 14,2022 at 07:26:19 UTC from IEEE Xplore. Restrictions apply.

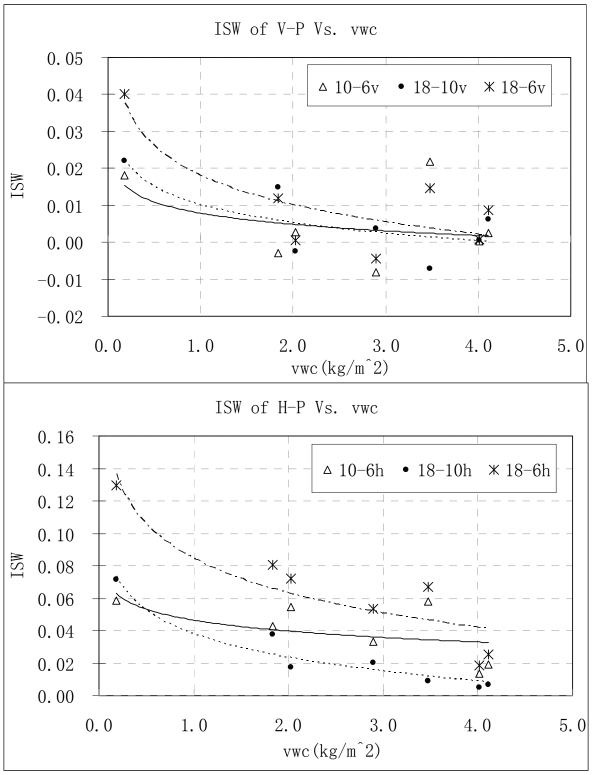

Fig. 5 Comparison of ISW calculated from various combinations of frequencies

Based on this finding, the ISW calculated from 18GHz and 6GHz horizontal polarization is selected in our algorithm.

Figure 6 shows a comparison of PI calculated from different frequencies. Black diamonds represent PI calculated from 6.9GHz; pink triangles for PI calculated from 10GHz and dark red cycles for 18GHz. It also very clear that the PI calculated from 6.9GHz has the largest variation range as the vegetation water content increases. And also PI calculated from 6.9GHz is selected in our algorithm.

IV. CONCLUSION

Spatial distributed soil moisture information is an essential parameter for hydrological, meteorological and ecological studies. Towards retrieving reliable soil moisture data from remote sensing observation, the vegetation effects should be identified firstly. The vegetation effects on the brightness temperature were studied through a long term winter wheat experiment. Through analyzing the experiment results at vegetated period, the vegetation effects on various frequencies were studied. The apparent emission over the winter wheat field measured by GBMRs at AMSR-E equipping frequencies increases as vegetation water content increasing from 0 to 3 kg/ m^2. Moreover, it is found that the heavy vegetation criterion is 2.0 kg/m^2 for frequencies higher than 18 GHz and is 4.0 kg/m^2 for all AMSR-E equipping frequencies.

An obvious application of this winter wheat microwave measurement is to support the development of land surface variables retrieval algorithm. As shown in section 3.C, basis on the synthetically analyzing the winter wheat experiment results, an AMSR-E soil moisture retrieval algorithm is decided to choose the PI of 6.9GHz and ISW calculated from 18GHz and 6.9GHz horizontal polarization to compose a look up table.

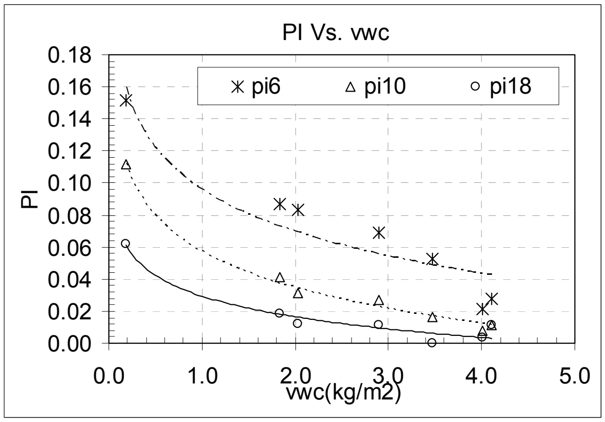

Fig. 6 Comparison of PI calculated from different frequencies

As a next step we will have to utilize this field experiment results to study the land surface process and land atmosphere interaction, by running the Land Data Assimilation System developed in the University of Tokyo (LDAS-UT) [5]. The multitemporal and multifrequency TB measurements and in situ observed meteorological forcing data and land surface variables will provide ample information for processing these studies.

ACKNOWLEDGMENT

This study was carried out as a part of Coordinated Enhanced Observing Period (CEOP) project funded by the Japan Science and Technology Agency and the Special Coordination Funds for Promoting Science and Technology. The authors express their so deep gratitude to them.

Furthermore we would like to thank UTFPSC, for providing us the possibility to conduct the field experiments in the university farm, Prof. Yonegawa and Mr. Kuboda for his helping in field management.

REFERENCES

[1] Eni G. Njoku, Thomas J. Jackson, Venkataraman Lakshmi, Tsz K. Chan., and Son V. Nghiem: Soil Moisture Retrieval From AMSR-E, *IEEE Trans. Geosci. Remote Sensing*, vol 41, pp. 215-229, February, 2003.

[2] Hui Lu, Toshio Koike, et al: A Basic Study on Soil Moisture Algorithm Using Ground-Based Observations under Dry Condition, JSCE, Vol. 50, Feb. 2006

[3] Technical documents of Radiometer Physics GmbH: Description 6 channel radiometer, Meckenheim, Germany. May, 1996

[4] T. J. Jackson and T. J. Schmugge: Vegetation Effects on the Microwave Emission of Soils, *Remote Sens. Environ.*, Vol. 36, pp. 203-212, 1991

[5] Kun YANG, Takahiro WATANABE, et al: An Auto-calibration System to Assimilate AMSR-E data into a Land Surface Model for Estimating Soil Moisture and Surface Energy Budget, *JMSJ*, Vol. 85A, pp 229-242, 2007.

Authorized licensed use limited to: Dedan Kimathi University of Technology. Downloaded on November 14,2022 at 07:26:19 UTC from IEEE Xplore. Restrictions apply.